

Hybrid Electron Beam Nanotechnology of Inorganic Material Deposition in Vacuum

B.A. Movchan,

*E.O. Paton Electric Welding Institute
68 Gorky str.
03150, Kyiv-150, Ukraine*

Currently available technological sequences of electron beam evaporation and subsequent condensation of inorganic materials are considered and new sequences are proposed, in particular, evaporation and reflection of the vapour flow using a reflector, as well as addition of active additives to the vapour flow of the main component, including gases, to trigger chemical reactions on the condensation surface in order to produce the respective micro- and nanostructures.

A general technological approach of “conservation” and storage of nanoparticles in an easily removable matrix has been proposed, in particular, to produce colloid systems. An example of a fluid with Fe₃O₄ magnetic nanoparticles is given.

A possibility of producing isolated (discrete) nanoparticles and nanostructures of ceramic materials and carbon is demonstrated.

It is noted that the physical method of material deposition from the vapour phase (PVD) and chemical deposition from the gas phase (CVD) have been combined on the basis of an electron beam heat source into a new technology complex for producing materials, namely “Electron beam hybrid nanotechnology of material deposition in vacuum”.

Keywords: electron beam evaporation, vapour phase condensation, thick films, coatings, nanomaterials, nanotechnology.

1. Introduction

Evaporation and condensation belong to fundamental physical processes of the world around us. Application of evaporation and condensation for producing and treatment of inorganic materials began comparatively recently, compared with many centuries of practical application of melting and solidification for these purposes. The ability to produce thin films by evaporation of metals in vacuum was demonstrated at the end of the 19th century [1]. The 30s of the previous century marked the start of application of electron beam heating for material evaporation in vacuum, i.e. start of electron beam technology of physical deposition from the vapour phase in vacuum (EBPVD).

In the following decades vacuum technologies of producing thin films (< 1 μm) were intensively developed – from antireflecting or reflecting optical coatings to a separate class of thin-film materials – the basis of modern microelectronics and computational and information technology. Synthesis of solid-state thin-film structures by a controllable laying of vapour phase atoms allowed creation of miniature devices with specific characteristics which seemed to be fantastic in the recent past.

At the start of the 60s of the previous century the E.O. Paton Electric Welding Institute began systematic research and development of equipment and electron beam technology of producing thick films (1 - 2 mm) of inorganic materials and studying their properties [1, 2]. Broad possibilities of “engineering” new inorganic materials and coatings were demonstrated in the case of thick composite condensates, and it was noted that technology of such a level of precision belongs to the category of modern nanotechnologies [3].

The business card of practical application of physical vapour phase deposition (EB-PVD) still are protective coatings on “hot parts” of gas turbine engines and other power units [4, 5].

At the same time, new experimental results have been accumulated on the technological capabilities of controlling the micro- and nanostructure of the condensates, in particular, by addition of active additives in the form vapour or gas into the main component vapour phase and realization of the respective chemical reactions on the condensation surface [6 – 8].

These results are generalized and briefly described below.

2. Electron beam evaporation

Electron beam evaporation of materials in vacuum differs from other methods of vacuum evaporation, namely thermic and ion-plasma- primarily by its versatility, technological flexibility and cost-effectiveness. The electron beam is one of the most effective heat sources. At collision of a flying electron with the solid surface, its kinetic energy is consumed in excitation of X-ray radiation, secondary emission and heating. At accelerating voltage of 20 – 25 kV and beam current of several amperes the energy loss for X-ray radiation excitation is equal to about 0,1% of the total power of the electron beam. X-ray radiation generated in the above voltage range, has a weak penetrability, and is completely absorbed by the metal walls of the chamber several millimeters thick. Energy losses for excitation of secondary emission (true secondary emission and reflected electrons) are equal to about 15%. The main part of kinetic energy of the electrons is converted into thermal energy in a thin surface layer of 1 - 2 μm thickness. Therefore, at heating by the electron beam the heat source is in the body proper and provides the maximum completeness of electric energy conversion into thermal energy.

Modern electron beam guns of 50 to 100 kW power allow evaporation of metal and non-metal materials with quite high rates, for instance up to $10^{-2} \text{ g} \cdot \text{cm}^{-2} \cdot \text{s}^{-1}$. At evaporation in vacuum of $10^{-4} - 10^{-6}$ Torr the spatial density of the vapour flow above the evaporator follows the cosinusoidal law of distribution, in keeping with which the maximum density is observed in the direction of the normal to the evaporation surface (angle $\alpha = 0$). At vacuum lowering to 10^{-2} Torr, for instance at introduction of argon or nitrogen into the chamber, the vapour flow is scattered in the direction of a more uniform density distribution. Evaporators consisting of a copper water-cooled crucible (cylinder), into which the evaporation material is placed in the form of an ingot (cast or compacted) of 25 to 70 mm diameter have become the most widely accepted.

Fig. 1 shows the schematic of such an evaporator. The level of the liquid pool surface is kept constant using a mechanism of vertical displacement of the ingot.

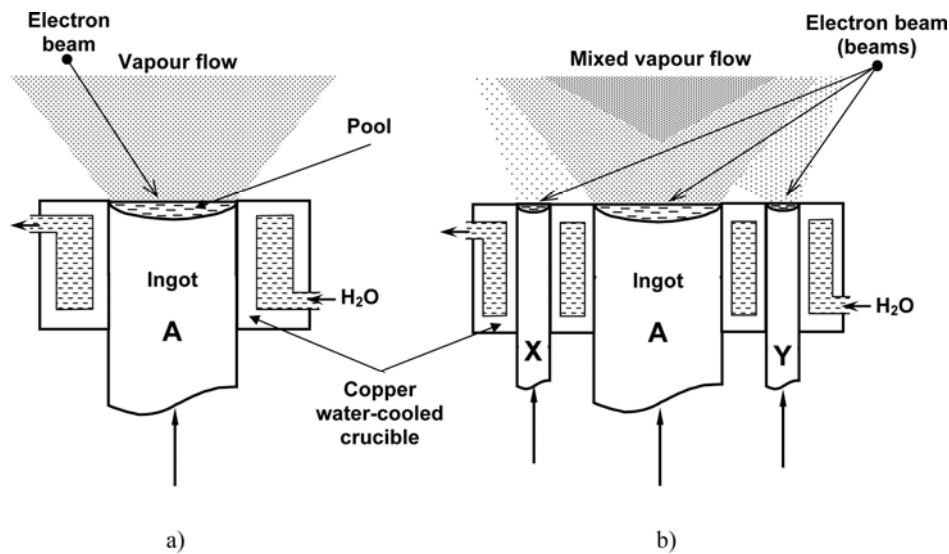


Fig. 1. Schematics of electron beam evaporation from copper water-cooled crucibles:
a) simple crucible; b) combined crucible

Maximum rates of ingot evaporation from a crucible of 70 mm diameter are equal, for instance to: iron – 3.0 kg/h, nickel alloys – 1.5 kg/h, graphite – 1.0 kg/h, ZrO_2 – 0.8 kg/h. Specific power consumption for the above materials is in the range of 15 to 40 kW·h/kg. Rate of vapour flow condensation on a flat stationary surface located above the pool surface at 300 mm distance from it, can be up to 30 – 50 $\mu\text{m}/\text{min}$ for metals and alloys, and 15 – 20 $\mu\text{m}/\text{min}$ ceramics (oxides, carbides, borides).

Fine drops appear in the vapour flow at high rates of evaporation of metals and alloys and respective overheating of the liquid pool surface. To eliminate this undesirable phenomena the so-called “hot” pool is used. Before the start of evaporation, a refractory metal tablet having a low vapour pressure at the ingot evaporation temperatures and not forming high-temperature intermetallics, for instance, niobium, is placed on the ingot end face, to make 30 – 40 vol.% of the future liquid pool. At the initial stage of ingot evaporation, a liquid pool is formed with a higher temperature and not prone to boiling. Under these conditions an increase of the evaporation rate of ingot material occurs with a practically complete absence of niobium or the drop fraction in the vapour flow. After evaporation of the entire ingot a “solid” pool (tablet) of Nb remains for further multiple application.

Another variant of the “hot” intermediate pool should be used at graphite evaporation. A tungsten tablet 4 – 5 mm thick is placed on the end face of the graphite ingot (rod). At heating first a liquid pool of tungsten is formed, and then a continuous process of solid graphite dissolution in liquid tungsten and its simultaneous evaporation from the liquid pool surface begins. Similar to the previous example, the tungsten tablet is reusable. Depending on the evaporation modes the carbon condensates can have up to 1 – 2 wt.% W.

There is also the need for a “cold” indirect heating by the electron beam to prevent overheating of the surface layer at evaporation of metals and alloys with a

low melting temperature, for instance In, Bi, Sn and their alloys; for a partial or complete prevention of pyrolysis and preservation of the initial molecular structure at evaporation of many inorganic and organic substances.

This condition can be easily met by using a simple device (reactor) in the form of a thick cover from refractory metals (Ta, Mo) or high-temperature alloys based on nickel or iron, located on the surface of a copper water-cooled crucible and heated by the electron beam. The specified system of holes in the cover will determine the spatial orientation of the vapour flow (see Fig. 3f). For many low-melting materials the water-cooled crucible case can be replaced by an uncooled one made of metallic materials, ceramics, graphite, not interacting with the evaporation material at the evaporation temperature.

Pure metals, similar to alloys, evaporate in the form of individual atoms. Some alloys, the components of which have close values of vapour pressure at the evaporation temperature, for instance Ni-Cr-Al, Ni-Fe-Cr-Al, can be evaporated from one source without variation of composition across the condensate thickness. For most of the alloys, however, the composition of the vapour phase above the melt does not correspond to the average composition of the melt. Alloy fractionation occurs: condensate layers adjacent to the condensation surface are enriched in the component with a high vapour pressure.

Condensates of multicomponent materials chemically uniform across the thickness, are produced by evaporation of components from independent sources, or using a combined crucible, Fig. 1b. A combined crucible is a copper block with a common water-cooling system of several cylindrical channels (crucibles) with a minimum wall thickness (3 - 4 mm) between them. Crucible of a maximum diameter (50 – 70 mm) is designed for the main ingot. Smaller diameters are for the other components.

Evaporation is performed by one or several scanning beams depending on the combination of evaporation materials. For instance, one beam is enough for the main ingot evaporation for combinations of metal, alloy or ceramics with a high melting temperature ($> 1000^{\circ}\text{C}$) for the main ingot and low-melting inorganic or organic materials for the other crucibles. Melting and evaporation of materials from the other crucibles will take place due to thermal energy of the liquid pool of the main ingot. At least two electron beams are required for a combination of refractory materials: the first electron beam for the main material, and the second scanning beam for the other materials. Upwards feed of ingots as they evaporate is performed by one common mechanism or individual mechanisms, depending on the specific requirements to the vapour flow composition during ingot evaporation.

Evaporation of compounds (oxides, carbides, borides, etc.) is, as a rule, accompanied by a change of the form of the initial molecules. Many high-melting compounds are characterized by partial dissociation of the initial molecules with formation of gaseous products, for instance, O, Al, AlO_3 and Al_2O form at Al_2O_3 evaporation. A reverse process can take place on the condensation surface, namely recombination and practically complete restoration of the initial composition and structure. High-melting oxides (Al_2O_3 , Y_2O_3 , ZrO_2 , MgO), carbides (TiC, ZrC, NbC, B_4C), borides (TiB_2 , ZrB_2) can be evaporated from copper water-cooled crucibles

using electron beam heating practically without any change of the composition. A number of compounds, for instance WC, TiN, cannot be deposited by direct evaporation, as at heating they decompose with formation of products with markedly different volatility. Such compounds in the form of condensates can be produced by evaporation of components from two independent sources, a combined crucible or using so-called reactive evaporation with bleeding nitrogen into the working chamber and vapour flow ionization.

Adjustable evaporation from one source of materials with different vapour pressure, for instance metals, ceramics, is possible using a composite ingot. Fig. 2 shows a schematic of a composite ingot structure. A composite ingot, preferably of a cylindrical shape, consists of a ceramic base and individual fragments (inserts) of metal and non-metal materials of the required shape and dimensions selected and arranged in the ingot volume so that at continuous evaporation and subsequent condensation of the vapour phase on the substrate a graded multilayer condensate of the specified composition and structure formed.

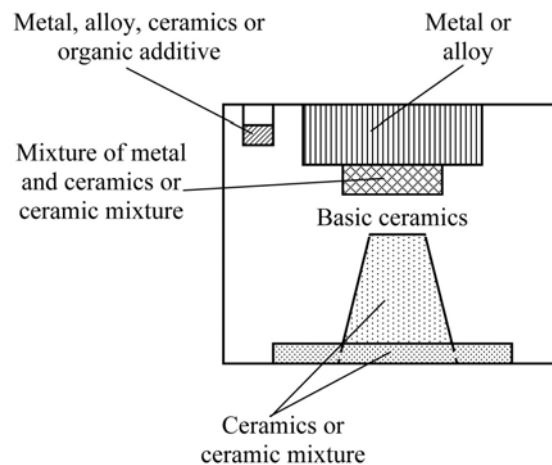


Fig. 2. Schematic of a longitudinal section of a composite ingot.

The ceramic base of the ingot determines the purpose of the graded coating. For instance, for thermal barrier coatings this is ZrO_2 with stabilizer additives or other oxide systems with low heat conductivity. For high-temperature coatings an Al_2O_3 ceramic base of the ingot is required. For hard coatings it should be from TiC, TiB_2 or B_4C .

Inserts located in the upper part of the ceramic ingot have the shape of small ingots (cylinders) or tablets and depending on the coating purpose they are made from pure metals, alloys, intermetallics, silicides, metal ceramics, ceramics or organic substances with the melting temperature below or vapour pressure higher compared to these parameters of the ingot ceramic base. These inserts are the first to evaporate at heating of the composite ingot and, while condensing, form transition bond coats on the substrate of the required composition and structure. The positive influence of low-melting metals and alloys present in these inserts should be noted, for instance, Al, the melting temperature of which is lower than that of substrate preheating before deposition of a thermal barrier coating. A thin liquid film formed on the substrate surface at the initial moment of their condensation, dissolves the microroughnesses of

the surface, and while interacting with the substrate material, promotes formation of the transition bond coat.

Additional cleaning of the condensation surface and its microalloying can be performed using inserts of organic substances, for instance anthracene ($C_{14}H_{10}$) with the melting temperature of $351^{\circ}C$ or Teflon (C_2F_4) with the melting temperature of $327^{\circ}C$.

Inserts located in the middle and lower parts of the ceramic ingot, have the form of tablets or cylinders with a cylindrical, conical or more sophisticated surface, and are made predominantly from ceramics, metal-ceramic or ceramic mixtures. Evaporating and condensing simultaneously with the ceramics of the ingot base, they form the composition, structure and properties of the ceramic layer (or layers) of the graded condensate.

The above evaporators, evaporation technique and examples of evaporation materials are applied in the up-to-date versions of electron beam hybrid nanotechnology and respective equipment.

3. Main technological schematics of material evaporation and condensation

Coming to consideration of the technological processes of evaporation and condensation it should be noted in particular that all of them are conducted in vacuum and are practically not accompanied by evolution of harmful vapours and gases into the environment.

Depending on the posed practical task, there exist different technological variants of material evaporation and condensation. Fig. 3 shows the technological schematics of evaporation and condensation from one source. Fig. 3a is simple evaporation and condensation on a flat substrate. It is natural that the condensation surfaces can also be cylindrical or of a more complex shape, stationary or can make certain displacements in space using the respective mechanisms of motion transfer. Fig. 3b is evaporation with vapour flow ionization by an arc discharge, using a circular electrode and application of a negative electric bias to the substrate. A vapour flow is formed with accelerated ions of the evaporation material, and, if required, of gases additionally bled into the vacuum chamber at the pressure of $\sim 5 \cdot 10^{-3}$ Torr, for instance nitrogen ions at titanium evaporation for synthesis of titanium nitride on the condensation surface. Fig. 3c is evaporation with irradiation of the condensate surface by ions of Ar or other gases using a magnetron ion source for controlling the condensate structure, in particular, controlling porosity. If required, a negative bias is applied to the substrate, similar to Fig. 3b. Fig. 3d is evaporation with subsequent reflection of the vapour flow with the purpose of changing its direction in space and controlling (decreasing or increasing) the energy of vapour flow atoms. At reflection of atoms (clusters) of carbon vapour flow, containing impurity atoms of tungsten, refining takes place. Surface of a reflector from W, Ta or Mo adsorbs tungsten atoms and simultaneously “cools” the reflected carbon atoms (clusters). Fig. 3e is evaporation and condensation on the inner cylindrical surface of the item. The gun and evaporator are located in a special device, capable of making reciprocal motion.

Fig. 3f is evaporation of low-melting inorganic materials and many organic materials from a reactor. In particular, solid hydrocarbons with controllable pyrolysis and formation of atomic-molecular vapour (gas) flow.

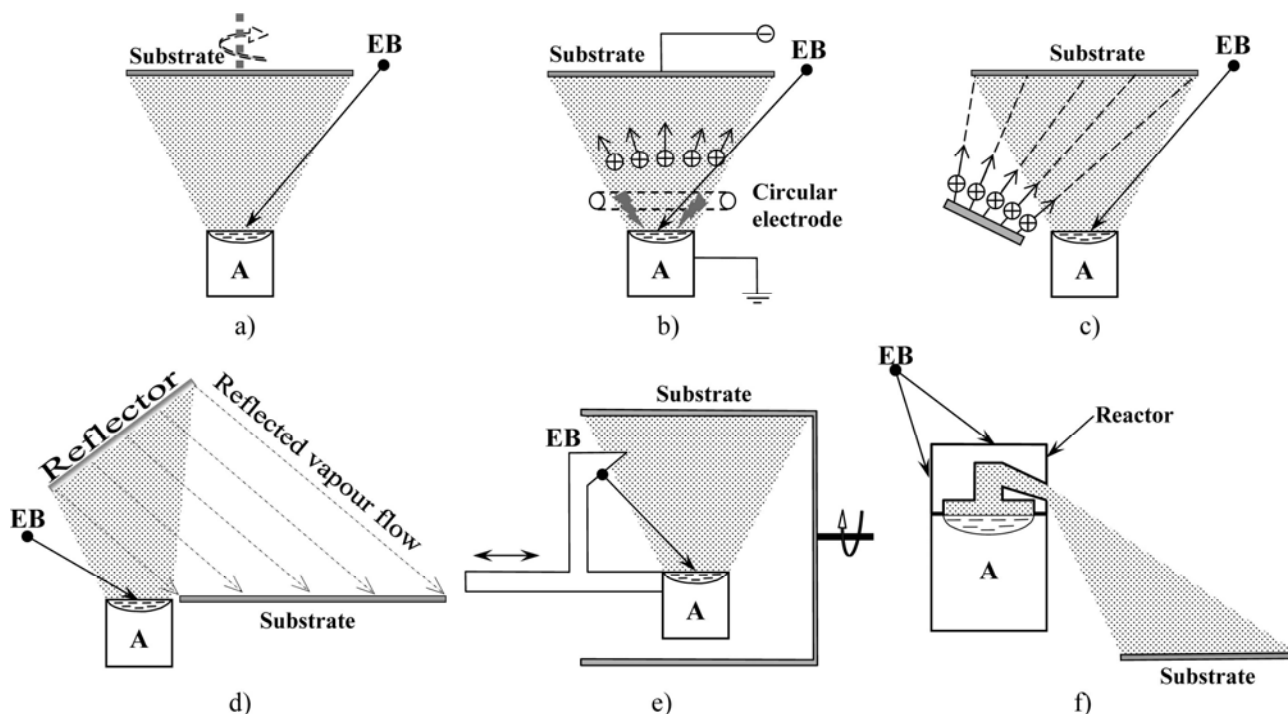


Fig. 3. Technological schematics of electron beam evaporation and condensation from one source.

It should be noted that the technological schematics in Fig. 3d and 4f demonstrate the possibility of changing the direction of vapour flows in space (downwards), this allowing, in particular, implementation of variants of condensation on flat liquid surfaces.

Fig. 4 shows some technological schematics of electron beam evaporation and condensation of materials from two and more sources.

Fig. 4a is evaporation from two independent sources and deposition of a mixed vapour flow on a stationary substrate. If material X is similar to material A, the condensate will have the same composition along the entire length of the substrate. If A and X are dissimilar materials, a gradient of composition $A \rightarrow X$ and respective structures forms along the condensate length. Fig. 4b is evaporation from two independent sources and deposition of mixed or separated by a partition (dotted line) vapour flows on a substrate of a circular shape rotating about a vertical axis. In the first variant, when $A = X$ or $A \neq X$ at a set rate of evaporation of materials A and X the condensate composition will be constant across the condensate thickness. In the presence of a partition and condition $A \neq X$ the condensate structure will become laminated. Layer thicknesses can be easily controlled by the speed of vertical shaft rotation at a constant rate of evaporation of A and X or by evaporation rate at constant rotation. It is quite obvious that the number of evaporators at realization of such technological variants can be increased to 3 – 4, if required. For instance, at

deposition of multicomponent condensates it is rational to apply two adjacent evaporators with materials A_1 and A_2 or X_1 and X_2 .

Fig. 4c is evaporation from two independent sources with subsequent reflection from reflectors and condensation on a substrate rotating around a vertical axis similar to the previous schematic in Fig. 4b. Distinctive features of this technological schematic compared to that in Fig. 4b consist in that the vapour flows are directed downwards. Therefore, conditions are in place for preservation of discrete condensation products (powders) on the substrate and, as noted earlier, there appears an additional possibility of deposition of vapour flows on flat liquid surfaces.

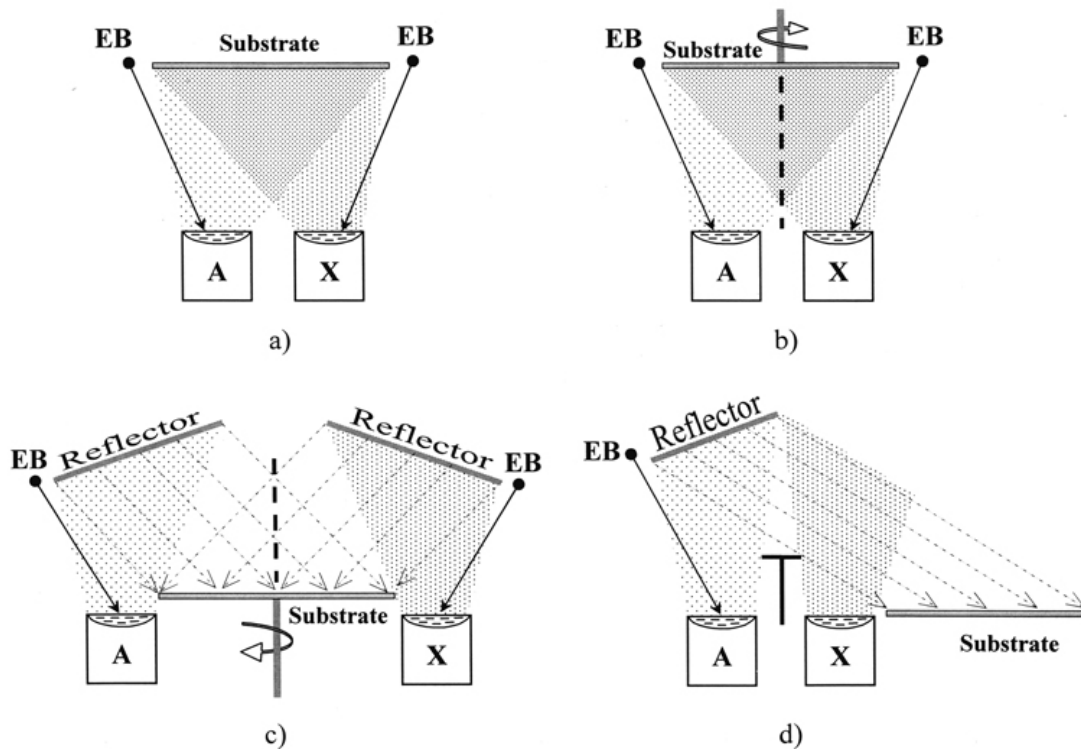


Fig. 4. Some technological schematics of electron beam evaporation and condensation from two and more sources.

Fig. 4d is evaporation from two independent sources. The first main flow of material A is reflected from the reflector in the direction of the condensation surface (solid or liquid). The second vapour flow of material X is not oriented towards the substrate, but just crosses the vapour flow of material A. In the zone of vapour flow crossing interaction of atoms, molecules or clusters of materials A and X occurs. After that the modified vapour flow A_x is deposited on the substrate.

Fig. 5 shows the technological schematic of evaporation of two materials from two independent sources with subsequent reflection and crossing of the vapour flows. In the zones of crossing and mixing of the vapour flows condensation processes can take place in the volume with formation of the respective nanostructures in the form of a deposit on the cooled surface.

Unlike the above variants the effectiveness of this variant needs to be checked experimentally. It should be added that other evaporator combinations can be applied

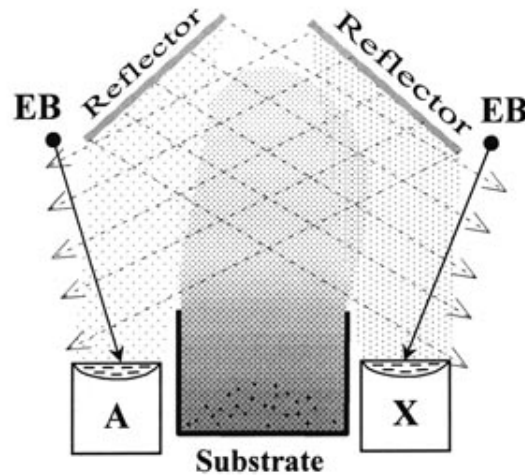


Fig. 5. Evaporation from two sources with reflectors and mixing of vapour flows for condensation in a volume.

to create potential zones of condensation in the volume, for instance a combination of the evaporator with a reflector (Fig. 3d) and reactor evaporator (“kettle”) – Fig. 3f.

4. Technological parameters of deposition and some mechanism of condensate structure formation

Substrate temperature T is one of the main parameters determining the thick condensate structure. Atoms (molecules) of the vapour flow having a certain kinetic energy, when meeting with the condensation surface, go into an adsorbed state and, while exchanging energy with the surface atoms, move jumplike over the surface. Surface temperature determines the level of thermal activation of the adsorbed atom and, as a consequence, number of jumps, probability of meeting, and interaction with other adsorbed atoms and formation of the respective atomic configurations.

It is experimentally established that at direct electron beam evaporation of pure metals, carbon, high-melting compounds of the type of oxides, carbides, borides and subsequent condensation of the vapour flow on the substrates in a broad temperature range T , three characteristic structural zones form with boundary temperatures T_1 and T_2 . Fig. 6 gives the schematic of structural zones depending on the homological temperature T/T_m (T_m is the melting temperature in Kelvin degrees). For instance, for pure nickel condensates the average values of boundary temperatures are equal to: $T_1 = 270^\circ\text{C}$; $T_2 = 450^\circ\text{C}$.

Based on estimation of the energy of activation of thermally activated processes in the above zones, an assumption is made on the main mechanisms controlling structure formation in each of them, namely a limited transition (jump) of atoms between two adjacent equilibrium positions on the condensation surface in the first zone; surface diffusion in the second zone and volume diffusion in the third

zone. Accordingly, in the low-temperature zone ($T < T_1$) the condensates have an amorphous or nano-sized structure. In the second zone ($T_1 - T_2$) the condensates are characterized by a columnar structure with a predominantly crystallographic

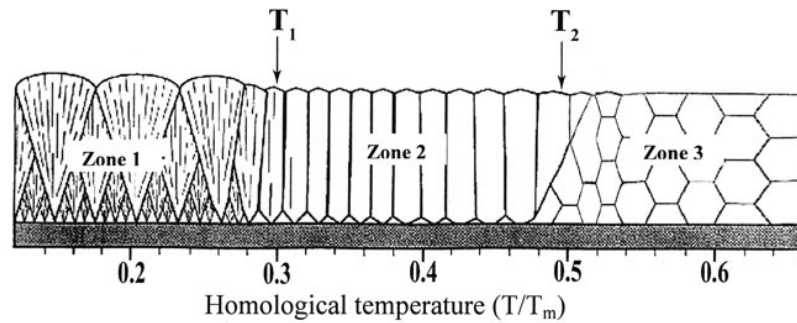


Fig. 6. Schematic of condensate structure.

orientation. The width of columnar crystallites increases from several tens of a micrometer to several micrometers with temperature increase in the range of $T_1 - T_2$.

Non-equilibrium structures in these zones are also characterized by nano- and microsized porosity, dependent on individual properties of materials, and technological parameters of deposition, primarily, on substrate temperature, deposition rate, orientation and motion of the substrate relative to the vapour flow.

In the high-temperature third zone ($T > T_2$) the columnar structure smoothly changes into an equiaxed grain structure. Grain size increases with temperature T . For instance, for pure nickel condensates at $T = 850^\circ\text{C}$ the average grain size is equal to $70 - 75 \mu\text{m}$.

It should be noted that T/T_m parameter characterizes the ratio of the energy of adsorbed atoms to the evaporated atom energy. Therefore, the change of the energy of evaporated atoms before meeting with the condensation surface will change the boundaries of structural zones T_1 and T_2 on T/T_m scale. For instance, at ionization and acceleration of the vapour flow ions T_1 will shift from 0.3 values towards 0.2.

It is characteristic that for materials, the adsorbed atoms of which weakly interact with the condensation surface, desorption is observed at $T/T_m > 0.75 - 0.80$. In particular, desorption of Cu, Ni, Fe, Ti atoms occurs from polished surfaces of Mo, W, Al_2O_3 .

Fig. 7 shows the dependence of critical temperature of complete interruption of condensation of the above elements on the substrate on their deposition rate.

These regularities allow development of vapour flow reflectors for concrete technological processes, the schematics of which are considered in the previous paragraph.

At deposition of multicomponent systems many elementary mechanisms of interaction of adsorbed atoms are manifested on the condensation surface. At the initial stage of nucleation and formation of condensation centers interaction of the adsorbed atoms with the substrate and with each other takes place, and further on - with each other and the incoming atoms of the vapour flow. Many variants of equilibrium and non-equilibrium atomic configurations with the near and far-range order and the respective structures of thick multicomponent condensates are possible.

Controlling the condensate adhesion to the substrate through the technological

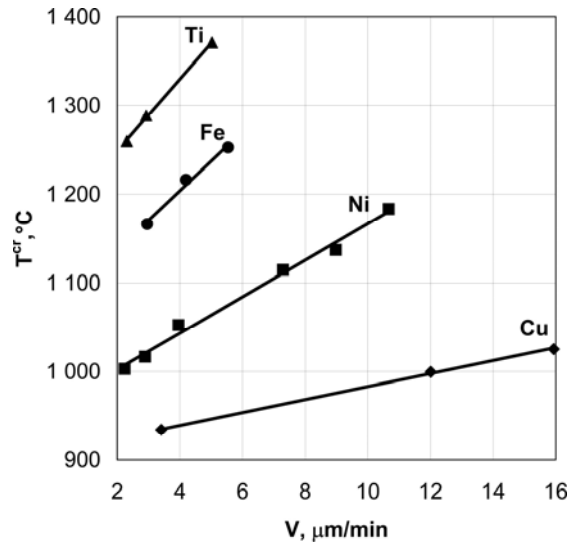


Fig. 7. Dependence of critical substrate temperature T^{cr} on condensation rate V .

parameters, it is possible to achieve a good bonding on the boundary or, contrarily, create the conditions for the condensate separation from the substrate.

5. Condensate structure

Technological experience has been accumulated so far of producing many single-phase and multiphase metal, metal-ceramic or ceramic condensates in a broad range of forms and dimensions of structural elements. “Structure – properties” dependencies are established [6 – 8].

Fig. 8 shows the structural schematics of these condensates. Dimensions of

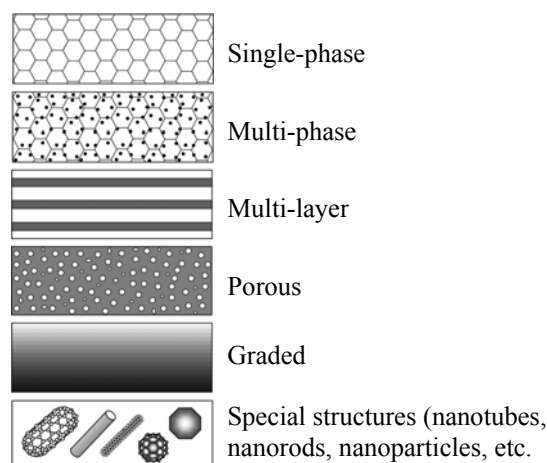


Fig. 8. Schematics of the structures of materials, produced by vapour phase deposition.

grains, phases, pores, particles, layer thickness can be varied in broad ranges: from several nanometers to several micrometers.

Substrate temperature and amount of the second phase (additive) are the main parameters for controlling the structure of two-phase condensates.

Fig. 9 shows the dimensions of ZrO_2 particles in Ni- ZrO_2 condensates, depending on ZrO_2 content at three condensation temperatures: 650°C, 850°C and 1100°C. Ni- ZrO_2 condensates 1.0 – 1.2 mm thick were produced by evaporation of Ni and ZrO_2 from two independent sources or using a combined crucible (see Fig. 4a and 1b). To study the structure and properties the condensates were separated from the substrate using to an anti-adhesion layer of CaF_2 1 – 3 μm thick, pre-deposited on the steel substrate.

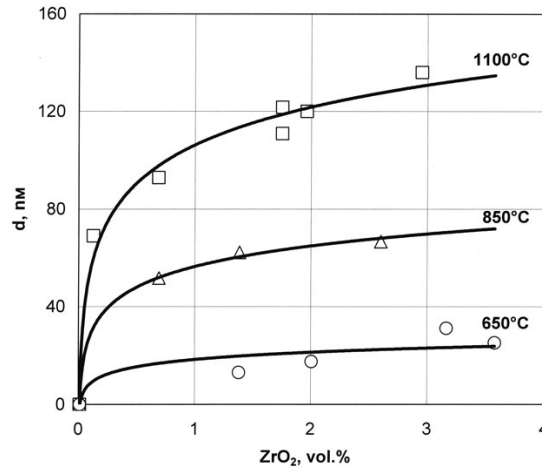


Fig. 9. Dimensions of ZrO_2 particles in Ni – ZrO_2 condensates at different substrate temperatures depending on ZrO_2 content.

As follows from the presented dependencies, the size of ZrO_2 nanoparticles increases with substrate temperature and volume content of ZrO_2 . At the temperature $T = 650^\circ C$ and content of 1.0 – 3.0 vol.% ZrO_2 the average particle size is equal to 20 – 25 nm. Increase of the amount of dispersed particles in the condensate is accompanied by a marked refinement of the nickel matrix grains.

For instance, the average grain size in pure nickel condensates at $T = 850^\circ C$, as was noted above, is equal to 70 – 75 μm , and at the same substrate temperature and content of 1.5 vol.% ZrO_2 it decreases to approximately 4.0 μm . Refinement of the size of grain (crystallites) occurs monotonically with increase of ZrO_2 content.

Similar regularities are also characteristic of other condensates of metal – high-melting oxide. High thermal stability of these compositions should be noted, for instance, in condensates with a matrix of nickel, iron and copper particle growth does not occur at heating up to temperatures of 0.9 T_m and soaking for 10 – 20 hours. They demonstrate a high level of mechanical properties with the characteristic dimensional effects [8].

As shown by experimental investigations the considered technology variant of simultaneous evaporation from two independent sources of the matrix material and a material not interacting with the matrix, and subsequent condensation of the mixed vapour flow can be quite effective when producing the so-called colloid systems, primarily, magnetic fluids.

These systems can be readily produced using a lost inorganic (or organic) matrix, in which nanoparticles of the second material were “reserved” initially by evaporation and condensation.

Fig. 10 shows magnetic particles of Fe_3O_4 from a water solution produced by a simple technology cycle: simultaneous evaporation of NaCl and Fe_3O_4 from two independent sources; subsequent condensation of a mixed vapour flow on a steel substrate; separation of the condensate from the substrate and its dissolution in water. Variation of substrate temperature in the range of 250 C allows smooth adjustment of the mean size of Fe_3O_4 particles from 2 to 15 nm. Particle stabilization is performed by standard methods, additives of biocompatible polymers (dextrin and polyvinyl alcohol).

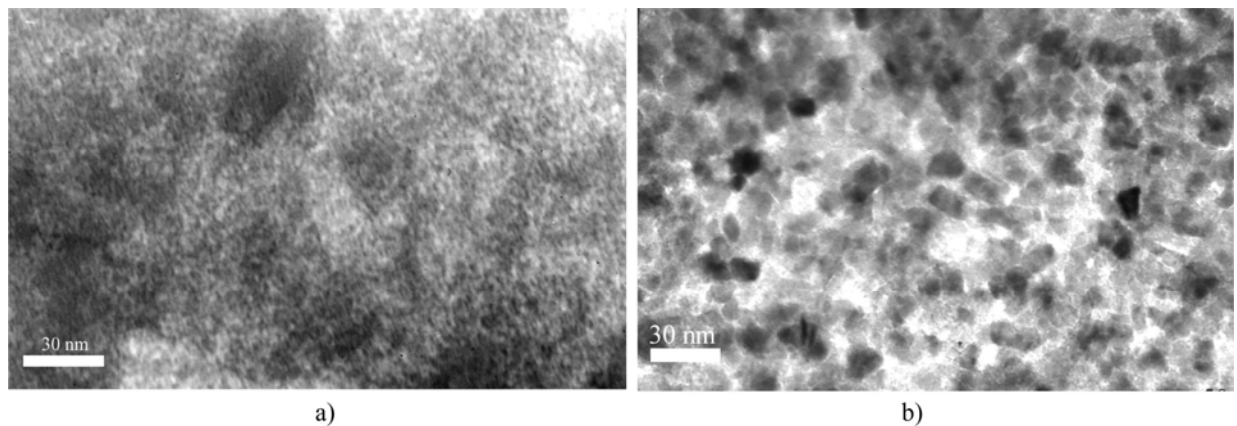


Fig. 10. Fe_3O_4 nanoparticles.

If required, Fe_3O_4 particles can be easily replaced by Ni, Co magnetic particles or their alloys, replacing Fe_3O_4 evaporation ingot by Ni or Co. It is also possible to “engineer” the bilayer nanoparticle by adding the respective additive, for instance, Cu, from an independent third source.

The next class is multilayer condensates. Figures 11a and 11b show the cross-sectional structures of thick multilayer condensates with alternating layers of TiAl

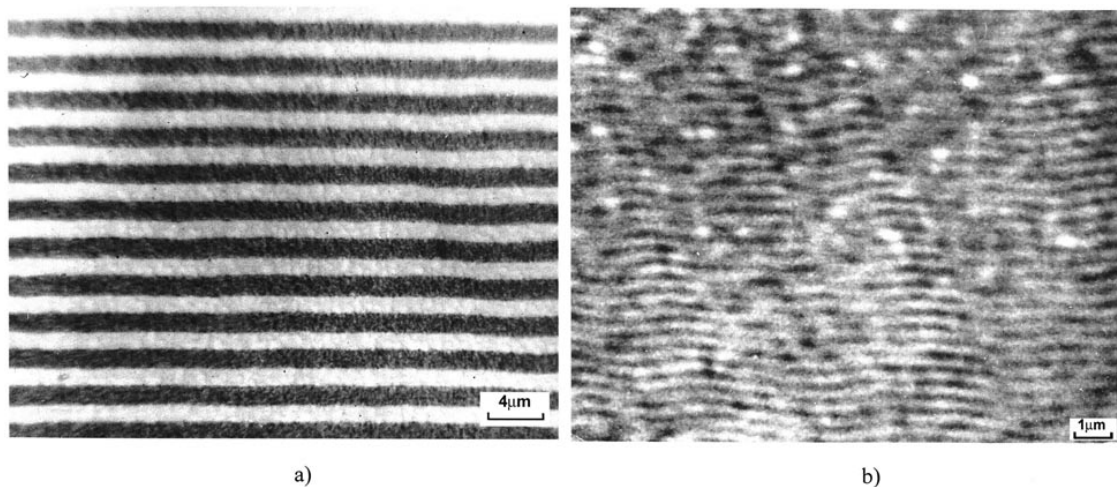


Fig. 11. Laminated TiAl/Ti structures.

and pure Ti of $\sim 1,2 \mu\text{m}$ and $0,15 \mu\text{m}$ thickness, respectively. The condensates were produced by the technology variant shown in Fig. 3b, without a partition. Ingot A is

titanium, ingot X is aluminum. Ti evaporation was continuous, that of Al was cyclic: switching on – off. Condensation was performed on the surface of a rotating disc of 480 mm diameter. Synthesis of TiAl intermetallic occurred in the cycle of simultaneous evaporation of Ti and Al and their subsequent condensation on the substrate. Ti layer was deposited in the cycle of switched off Al feed.

Dimensional effects of the mechanical properties, primarily strength and hardness, are manifested in condensates with layer thickness less than 1 – 2 μm . The interfaces between the layers are effective barriers in the path of moving dislocations. For this reason multilayer condensates demonstrate a high level of strength at room and high temperatures [3, 8].

Heat conductivity and thermal expansion can be also controlled by appropriate selection of materials and layer thicknesses.

Non-equilibrium processes of evaporation and condensation of inorganic materials allow producing a wide class of porous materials. There exist a number of mechanisms and conditions of porosity formation at non-equilibrium condensation of the vapour phase. One of the main mechanisms of porosity formation is based on the so-called “shadowing” mechanism. During initiation and subsequent growth of different crystallographic faces of the nuclei with different rates, a certain relief forms on the surface. The faces and protrusions growing at the maximum rate, shield the adjacent surface regions from the evaporator (vapour flow). This results in formation of inner voids. The “shadowing” effect is enhanced, if the angle of incidence of the vapour flow on the condensation surface is below 90° , for instance at rotation of the cylindrical condensation surface about a horizontal axis. In all the variants, when a relief due to nucleation and growth of second phase particles, surface erosion at irradiation by accelerated gas ions, chemical reactions with removal of reaction products forms on the surface, a porous structure is produced [7].

Fig. 12a shows a cross-sectional structure of porous Ni – 16 wt.% $\text{ZrO}_2(7\text{Y}_2\text{O}_3)$ condensate of 420 μm thickness deposited on a stationary substrate at $T = 1100^\circ\text{C}$

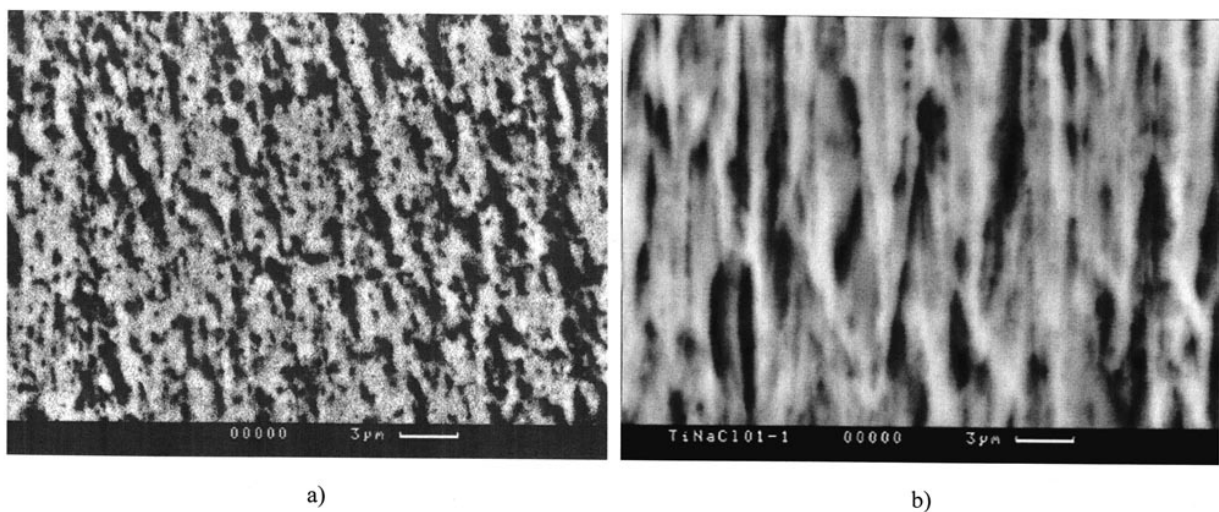
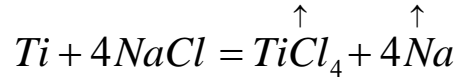


Fig. 12. Structures of porous condensates of Ni – 16 wt.% $\text{ZrO}_2(7\text{Y}_2\text{O}_3)$ (a) and pure Ti (b).

from two independent sources. $\text{ZrO}_2(7\text{Y}_2\text{O}_3)$ particles not interacting with the matrix, provide the “shadowing” effect and the respective porosity. Such a porosity forms in

metal (alloy) - oxide or oxide - oxide condensates with more than 15 – 20 wt.% oxide content, for instance: NiCrAl – Al₂O₃; NiCrAl – ZrO₂; ZrO₂ – Al₂O₃. At this concentration of oxides the pore size increases with substrate temperature.

Fig. 12b shows the structure of a porous titanium condensate 120 μm thick produced by deposition of a mixed vapour flow of Ti and NaCl. Etching of the condensation surface proceeds, primarily, of crystallite boundaries, with removal (evaporation) of the reaction products (shown by arrows):



NaCl and pure Cl are active additives forming easily removable gaseous chlorides at simultaneous condensation with Al, Ti, Si, ZrO₂, Al₂O₃, TiO₂.

Further adjustment of the porous condensate structure can be performed using capillary impregnation by the liquid phase during the condensate formation or directly after its deposition. “Refractory metal – liquid metal additive” or “refractory ceramics – liquid metal additive” compositions are characterized by formation of metal phase segregations along the crystallite boundaries as a result of capillary impregnation and accelerated mass transfer along the defective crystallite boundaries.

Fig. 13 shows the cross-sectional microstructure of a condensate of titanium carbide (TiC) 110 μm thick deposited on a steel substrate heated up to 1000°C. At the

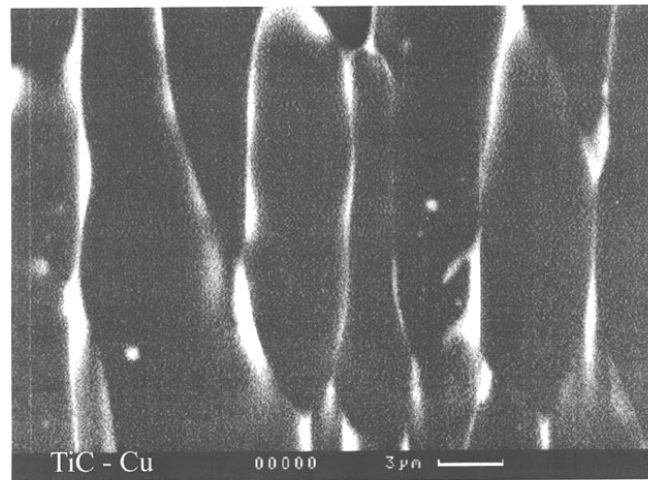


Fig. 13. Structure of copper-impregnated TiC condensate.

final stage of deposition a copper additive in the amount of about 10 wt.% is introduced into TiC vapour flow from an adjacent source. As follows from the microstructural pattern simultaneously with deposition of the upper TiC + Cu layer Cu penetrated along the boundary zones of columnar crystallites to the entire condensate thickness. Time of the final deposition stage is equal to 2 – 3 minutes. The width of intercrystalline copper interlayers is less than 0.2 μm.

It is experimentally established that small additives (4 – 5 vol.%)Cu practically do not affect the value of TiC and TiB₂ condensate microhardness, but lower the brittle fracture susceptibility.

A characteristic example of a graded metal-ceramic condensate can be a graded thermal barrier coating with an outer ceramic layer deposited using a composite ingot (see Fig. 2) [5, 6].

Figures 14a and 14b show the schematic of a variant of a composite ingot, distribution of the content of chemical elements by weight across the section of graded thermal barrier coating and cross-sectional structure of the coating produced

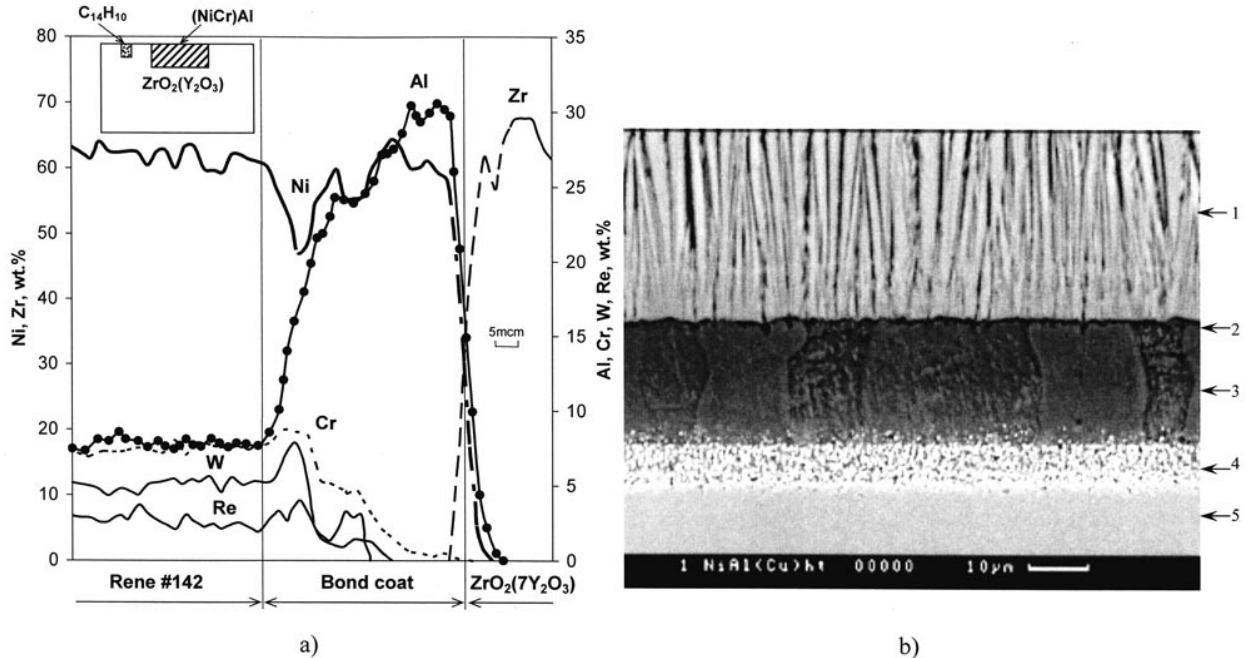


Fig. 14. a) schematic of a longitudinal section of $ZrO_2(7Y_2O_3)$ composite ingot with inserts of $C_{14}H_{10}$ and $(NiCr)Al$ alloy and distribution of chemical elements over the coating section, b) coating structure: 1 – $ZrO_2(7Y_2O_3)$; 2, 4 – transition zones; 3 – $NiAl$; 5 – substrate (blade surface).

by continuous evaporation of this ingot. A composite ingot of 68 mm diameter had a ceramic base of $ZrO_2(7\%Y_2O_3)$ and two inserts: $NiAl$ intermetallic of 45 mm dia. produced by pre-sintering of powders, and anthracene $C_{14}H_{10}$ in the form of 10 mm diameter tablet. Coating of the total thickness of $150\ \mu m$ is deposited on the surface of Rene 142 alloy at surface temperature of $950^\circ C$ by direct electron beam evaporation of the ingot. After deposition, annealing of the sample with a coating was performed in a vacuum of approximately 10^{-4} Torr at $1080^\circ C$ for 1 h for stabilization of the coating structure.

As follows from comparison of the figures, the coating consists of a bond layer of $NiAl$ intermetallic, two transition zones and upper ceramic layer of $ZrO_2(7\%Y_2O_3)$ with a columnar structure and columnar intercrystalline porosity.

The fatigue life of such graded coatings deposited in one process cycle is approximately 2.0 – 2.5 times higher and the cost is lower compared to the traditional multistage coatings.

A vast class of highly porous condensates with practically isolated from each other structural elements of different shapes and dimensions should be also singled out.

There exist two main technological variants of producing such discrete structures: condensation on a substrate and condensation in a volume with subsequent gravity-induced deposition of the product on the substrate (see Fig. 5). Examples of isolated structures produced on a substrate, will be considered below. The mechanisms of these structures formation are largely similar to those of porous structure formation. For condensates with isolated structural elements, particularly of small thicknesses (1 – 3 μm), the composition, crystalline structure and relief of the substrate are important.

A new technological variant of producing isolated discrete structures is condensation of the main material on the substrate in the vapours of the reflected and not interacting with the main material second component, which has a high vapour pressure and is evaporated from an adjacent source, for instance In, Sn, Bi metals. In a specific case, these are neutral gases Ar or He added to the main vapour flow and reflected by the condensation surface.

Figures 15 – 17 give examples of such structures.

Fig. 15 gives the microstructures of highly porous $\text{ZrO}_2(7\text{Y}_2\text{O}_3)$ and $\text{ZrO}_2(15\text{Y}_2\text{O}_3)$, condensates deposited on a polished surface of iron with practically isolated structural elements.

Fig. 15a is $\text{ZrO}_2(15\text{Y}_2\text{O}_3)$ condensate with 7.0 wt.% Zr. Deposition temperature is 900°C.

Fig. 15b is $\text{ZrO}_2(7\text{Y}_2\text{O}_3)$ condensate with addition of NaCl vapour phase from an independent source into the main vapour flow of $\text{ZrO}_2(7\text{Y}_2\text{O}_3)$. Deposition temperature is 900°C.

Fig. 15c is $\text{ZrO}_2(15\text{Y}_2\text{O}_3)$ condensate deposited in a re-evaporated flow of indium. Deposition temperature is 700°C. Granules with inner nanopores.

Fig. 15d is $\text{ZrO}_2(7\text{Y}_2\text{O}_3)$ condensate deposited in a re-evaporated flow of tin. Deposition temperature is 950°C.

Fig. 16 shows the microstructures of Al_2O_3 condensates deposited on a polished surface of iron.

Fig. 16a is a condensate of pure Al_2O_3 . Deposition temperature is 940°C, α - Al_2O_3 structure.

Fig. 16b is Al_2O_3 condensate with addition of NaCl vapour phase from an independent source into the main Al_2O_3 flow. Deposition temperature is 900°C.

Fig. 17 gives the structures of carbon condensates.

Figures 17a and 17b are tubular structures produced on a polished surface of iron in the range of 100 – 250°C at evaporation and partial pyrolysis of anthracene ($\text{C}_{14}\text{H}_{10}$) using a reactor (see Fig. 3e).

Figures 17bc and 17d are rod structures produced on a polished and then oxidized surface of iron, also in the range of 100 – 250°C. Carbon evaporation was performed from a tungsten pool with subsequent reflection of the vapour flow (see Fig. 3d).

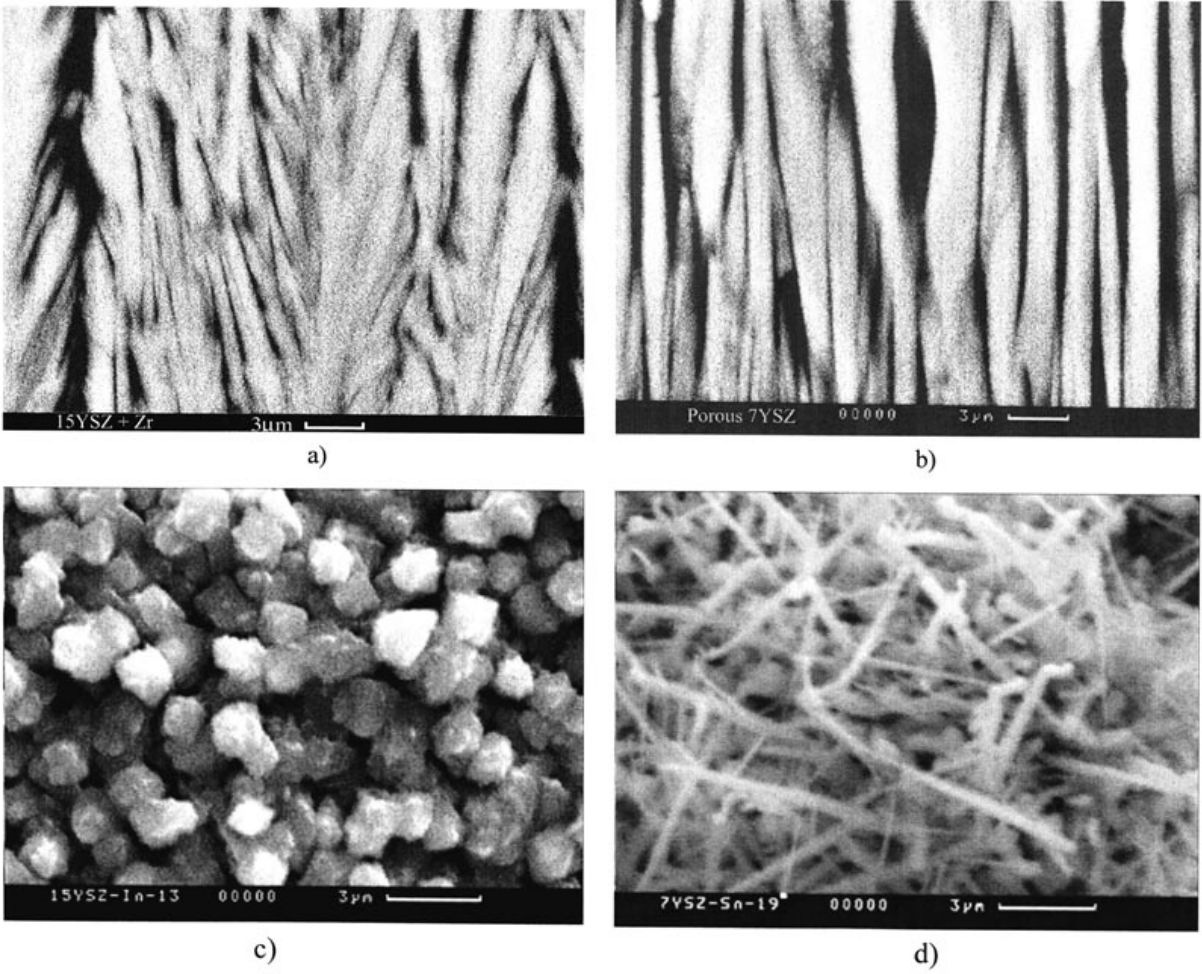


Fig. 15. Structure of condensates of ZrO₂ oxide.

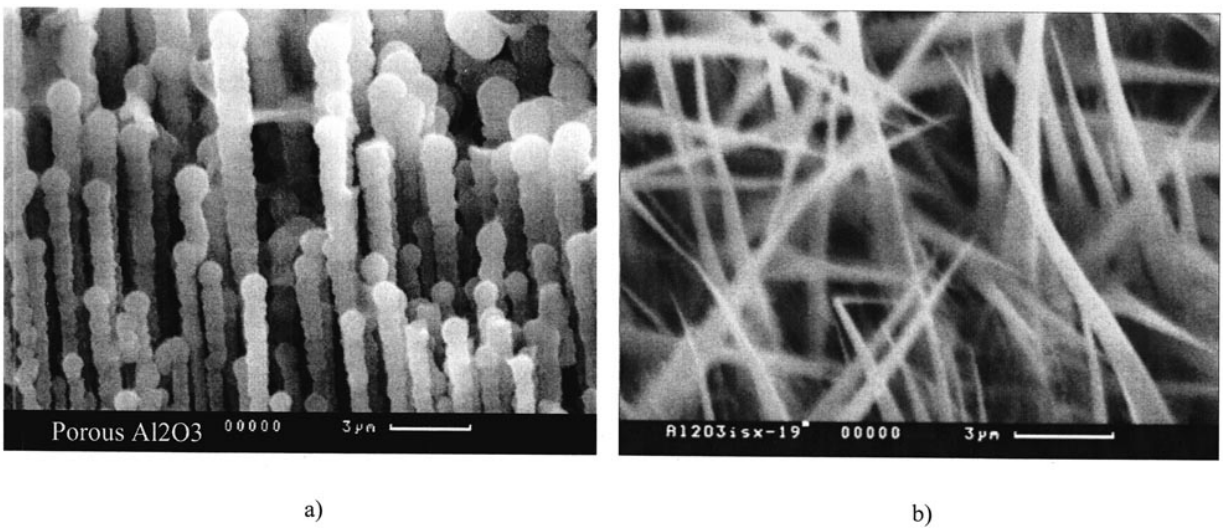


Fig. 16. Structure of condensates of Al₂O₃ oxide.

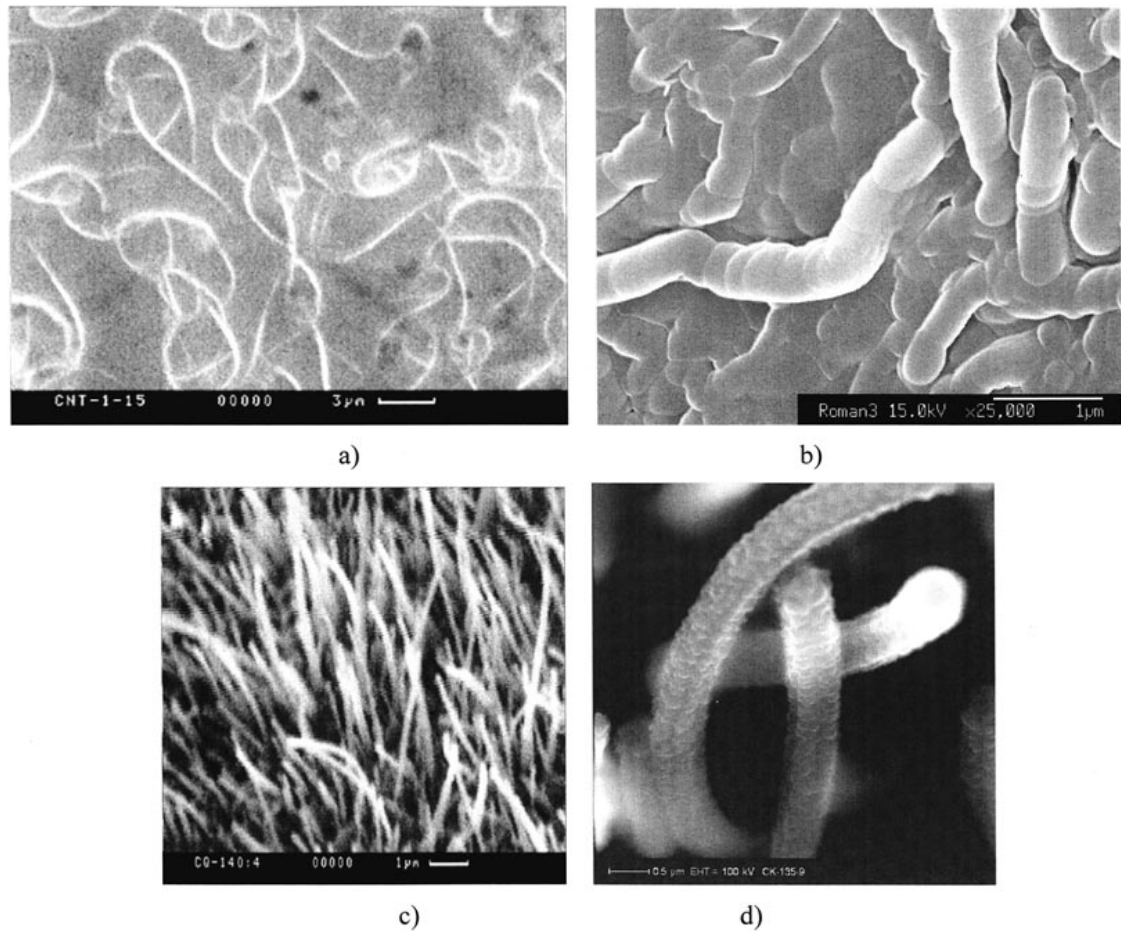


Fig. 17. Structure of carbon condensates.

6. Equipment

The International Center for Electron Beam Technologies of the E.O. Paton Electric Welding Institute developed and organized manufacturing of laboratory, pilot-production and production electron beam equipment for realization of the considered variants of technological processes.

Electron beam units of 150 and 250 kW power have a working chamber, one or two load chambers, vertical and horizontal shafts and respective manipulators for fastening the substrate and products.

The units have 4 or 6 electron beam guns of 40 – 60 kW power, differential vacuum system, up-to-date multiprocessor system of monitoring and control of the technological process of evaporation and condensation.

The main components of the units are Western made.

Fig. 18 shows the general views of the laboratory and pilot-production units. More than 10 units have already been manufactured for universities, scientific centers and industrial enterprises of the USA, China, Canada and India.

The International Center for Electron Beam Technologies is also training specialists for operation of electron beam units, fulfills joint research projects in the field of electron beam technologies.

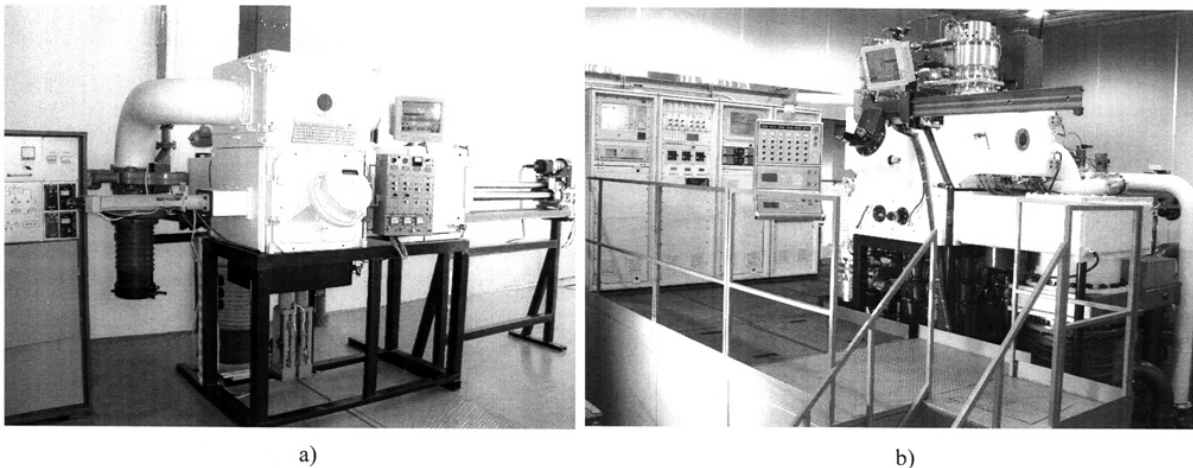


Fig. 18. General view of laboratory UE-209 (a) and pilot-production UE-204 (b) electron beam units.

7. Conclusion

The physical method of material deposition from the vapour phase (PVD) and chemical deposition from the gas phase (CVD) were combined on the basis of an electron beam heat source. A new technology complex for producing materials has been formed, namely “Electron beam hybrid nanotechnology of material deposition in vacuum”.

Electron beam hybrid nanotechnology is capable of filling a niche between the “thin-film” and traditional technologies of production of materials and items. The main feature of the new technology will be performance of solid-state synthesis of a specified sequence of structures, the totality of which will make the new product. Similar to “thin film” technology for many variants of products it will be possible to eliminate the traditional stages of production, namely initial fabrication of semi-finished products, for instance, fine powders, their further processing and fabrication of individual parts, and, finally, their joining to form a new product.

Electron beam hybrid nanotechnology and the respective equipment are a real basis for further scientific-technical progress of economy in production of materials, coatings and products:

Functional coatings:	Structural coatings and items:	Materials and semi-finished products:
<ul style="list-style-type: none"> • Oxidation and corrosion resistant; • Thermal barrier; • Hard; • Wear- and erosion-resistant; • Damping; • Antifriction; • Coatings with special properties (biological, electric, magnetic, etc.). 	<ul style="list-style-type: none"> • Items with inner channels (gas turbine blades, etc.); • Elements of solid oxide fuel cell (SOFC) structures; • Carriers for catalysts, catalysts and catalysis devices; • Laser mirrors; • Filters; • Sorbents; • Medical equipment 	<ul style="list-style-type: none"> • Ceramic composite materials for operation at high temperatures ($T > 1600^{\circ}\text{C}$); • Metal and metal-ceramic micro- and nanolayered foils; • Consolidated and isolated nanostructures of carbon and its compounds; • Nanostructures (particles) of different materials preserved in the solid or liquid matrix, removable if required; • Magnetic nanofluids.

Reference

1. R.F. Bunshah. Vacuum Evaporation – History, Recent Developments and Applications. *Zeitschrift für Metallkunde*. 1984, v.75, No11; p.840 – 846.
2. R.F. Bunshah (editor). “Handbook of Deposition Technologies for Films and Coatings: Science, Technology and Applications”. Blue Ridge. (NJ): Noyes Publication, 1994.
3. B.A. Movchan. Composite Materials Deposited from Vapour Phase in Vacuum. *Surface and Coatings Technology*. 1991, v.46, p.1 – 14.
4. B.A. Movchan. EB-PVD Technology in the Gas Turbine Industry: Present and Future. *JOM*. November, 1996, p.40 – 45.
5. B.A. Movchan, K.Yu. Yakovchuk. Graded thermal barrier coatings, deposited by EB-PVD. *Surface and Coatings Technology*, 2004, v.188-189, p.85 – 92.
6. B.A. Movchan. Functionally graded EB-PVD Coatings. *Surface and Coatings Technology*, 2002, v.149, p.252 – 262.
7. B.A. Movchan, F.D. Lemkey. Some Approaches to Producing Microporous Materials and Coatings by EB-PVD. *Surface and Coatings Technology*, 2003, v.165, p.90 – 100.
8. B.A. Movchan. Inorganic materials and coatings produced by EBPVD. *Surface Engineering*, 2006, v.22, No1, p.35 – 46.